MM Science Journal | www.mmscience.eu
ISSN 1803-1269 (Print) | ISSN 1805-0476 (On-line)
Special Issue | HSM 2025
18th International Conference on High Speed Machining
October 15-16, 2025, Metz, France
DOI: 10.17973/MMSJ.2025_11_2025136

HSM2025-44819

INVESTIGATION OF COOLING EFFICIENCY AND STRUCTURAL CHARACTERISTICS OF SUPERCRITICAL CO_2 JETS FOR MACHINING ASSISTANCE

M. El Nahas[1,3]*, T. Pottier[1], J. J. Letourneau[2], Y. Landon[3]
[1]IMT Mines Albi, Clement Ader Institute, Albi, France
[2]IMT Mines Albi, RAPSODEE, Albi, France
[3]University of Toulouse, Clément Ader Institute, Toulouse, France
*Maha El Nahas; e-mail: maha.el_nahas@mines-albi.fr

Abstract
In a context of safer, more cost-effective, and environmentally friendly machining processes, supercritical carbon dioxide (sCO_2) emerges as a promising alternative to conventional cutting fluids. However, a consolidated understanding of the optimal sCO_2 jet parameters for machining and its impact on the tool and the material remains unavailable. This work intends to address the behavior of a free and impinged sCO_2 jet structure and its geometrical evolution in function of the upstream jet conditions. The supersonic structure and parameters were analyzed under varying initial pressures and temperatures in both near and far fields. The obtained images showed the detailed jet structure and highlighted the presence of three different zones within the flow: laminar, transitional then turbulent. To investigate this behavior and to better understand the jet's cooling ability in these different zones, an in-depth analysis of the jet's complex structure was carried out using high-speed imaging combined with an optical imaging known as Schlieren.

Keywords:
Schlieren imaging, Machining assistance, Green-manufacturing, Under-expanded Jet, Jet structure, Supercritical Carbon Dioxide, Near Field, Jet impingement

1 INTRODUCTION

In the literature, few studies addressed the thermal effect of the sCO_2 assistance and its efficiency to control the temperature within the cutting zone [Koulekpa 2023]. Results have shown a strong influence of the geometrical aspects of the CO_2 delivery, in terms of distance, angle, and shapes of either the nozzle and the cutting zone [Masson et al. 2025].

Kim and Lee [Kim 2019] have experimentally shown that « the cooling performances of supersonic impinging jets in the stagnation region are highly related to the jet flow field structures ». Although worthy of interest, such literature does not yet bridge the gap between the cooling capacity of the jet and the upstream thermodynamic conditions.

Experimental work has addressed the thermal condition of the impingement of such jet, but the literature remains largely incomplete when it comes to the geometry of the jet itself. All in all, strong academic knowledge of the thermodynamics of CO_2 is available, unlike the jet geometry and characteristics caused by such a discharge. This gap prevents any straight forward attempt to model the cooling resulting from such discharge.

The jet created by sCO_2 discharge is mostly characterized by a very high Nozzle Pressure Ratio $NPR = P_0/P_\infty$ (where P_0 is the stagnation pressure in the tank and P_∞ is the ambient pressure). Recalling that the critical pressure of CO_2 is 73.8 bar, the NPR resulting from such discharge in industrial context is typically above NPR > 100 [Supekar et al. 2012] and thus inevitably leads to a supersonic, extremely under-expanded jet. Consequently, a complex pattern of shock wave is created across a few diameters distance downstream the orifice.

In order to provide future model developments with valuable data, this paper intends to address the influence of the jet operating parameters P_0 and T_0 on the downstream geometrical structure of the expanded free and impinged jet.

In the context of sCO_2 assisted machining, the Near Field (NF) region of the jet, where the barrel shock structure develops, is of particular interest due to its pronounced thermal and geometrical effects. Located immediately downstream of the nozzle exit, this region exhibits significant pressure and temperature gradients, with a high-speed core surrounded by the curved surface of the barrel shock. This dynamic zone dictates how the jet expands and interacts with its surroundings, strongly influencing the way heat is transferred to the target surface.

In machining, and specially in drilling, the targeted surface is very close to the nozzle exit, making the NF zone of a large interest to investigate. This leads to an optimization of the the upstream jet conditions in order to get the best cooling efficiency of the sCO_2 jet for these applications.

2 SCO_2 COOLING ABILITY AND HEAT TRANSFER COEFFICIENT

The experimental work of Masson et al. [Masson et al. 2025] addressed the thermal condition of the impingement of such sCO_2 jet. The literature remains largely incomplete when it comes to the geometry of the jet itself thus preventing any straight forward attempt to model the cooling resulting from such discharge. In their study, the authors addressed the jet impingement on a hot metallic plate with the intention to evaluate the heat transfer coefficient (denoted h) for various operating parameter namely: the impinging angle, the plate to nozzle distance and the initial jet pressure P_0 and temperature T_0. Under the hypothesis that *"the solid phase does not contribute to the cooling differently than the vapor phase",* they provided with a rough approximation the heat exchanged between the jet and the plate surface which reads:

$$\boldsymbol{h}(\boldsymbol{x}) \propto \boldsymbol{\rho}(\boldsymbol{x})^{\boldsymbol{a1}} \times \boldsymbol{C_p}(\boldsymbol{x})^{\boldsymbol{a2}} \times \boldsymbol{V}(\boldsymbol{x})^{\boldsymbol{a3}} \qquad (1)$$

Where the a_i are experimentally adjusted parameters, ρ and C_p are the flow density and specific heat respectively and $V(x)$ is the local stream velocity. From such formalism it can be concluded that when impingement occurs at long range, these fields naturally regularize and averaging becomes reasonable. However, when impinging at very short distance, as it is the case in machining application (especially in drilling), the supersonic jet structures and the gradients which results from it are to be accounted for. The spatial heterogeneity of these fields, in the case of highly under-expanded jets, prevents from drawing any valid conclusion (even in terms of trends) from the above equation and thus points the need for further knowledge collection of the early structure of micro-supersonic jet of CO_2 which is the intention of the present contribution.

3 STRUCTURE OF A FREE SCO_2 JET

3.1 Highly under-expanded jet structure

In the investigated pressure and temperature range, the rapid expansion of sCO_2 can be considered strictly isenthalpic prior impingement. Assuming that the exit pressure P_e is always above three times the ambient pressure P_∞ under such operating conditions, the jet exhibits a structure known as highly under-expanded jet structure [Crist et al. 1966]. As represented in *Fig. 1* the number of shock cells is restricted to one and is dominated by the first cell, corresponding to the Mach disk. Supersonic expansion and re-compression zones can be observed behind the shock cell and tend to fade as the NPR increases. The flow is choked, and therefore a sonic line exists near the nozzle.

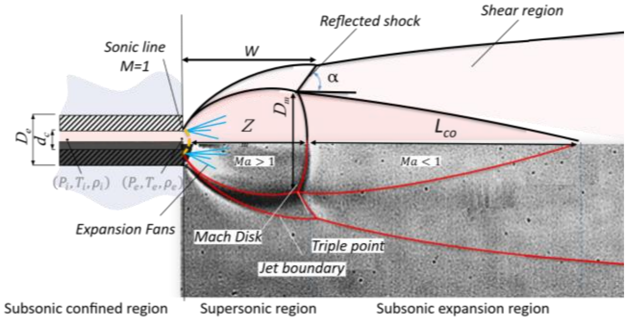

Fig. 1: Scheme of the Jet structure and characteristic parameters

The effect of the initial supercritical conditions on the free jet structure was investigated by analyzing Schlieren images obtained by each test for multiphase flow and single-phase flow. The characteristic dimensions of the Mach disk are:

- Mach disk position Z_m.
- Mach disk diameter D_m.
- Reflected shock angle α.
- Primary wavelength W.
- Mach disk area.

Most of these features have been the topic of dedicated studies, the review of which yields valuable insight into the geometry of highly under-expanded jet represented in *Fig. 1*. However, as stated in the review proposed by Franquet et al. [Franquet et al. 2015], the vast majority of those works address either species other than sCO_2 (Air, H_2, N_2, CH_4 or air+fuel) or lower NPR.

3.2 Experimental Setup

sCO_2 delivery apparatus

In this study, carbon dioxide is brought to a supercritical state through a sequence of controlled thermodynamic transformations involving cooling, pressurization, and heating. Initially stored in CO_2 cylinders, the gas is cooled to 2 °C to prevent cavitation during compression by a high-pressure pump. It is then pressurized and passed through a submerged coil in a thermostatically controlled oil bath to reach the target inlet temperature (T_0). The sCO_2 is subsequently expanded freely into ambient air through a capillary tube of 0.25mm diameter. The experimental setup, which includes a continuous high-pressure pump, a recirculating chiller, and a cylindrical coil heat exchanger, allows precise control of pressure and mass flow rate via a programmable logic controller and Coriolis flow-meter feedback. The investigation focuses on the flow behavior of sCO_2 jets under highly under-expanded conditions, with nozzle pressure ratios ranging from 80 bar to 220 bar and inlet temperatures between 323 K and 393 K.

Schlieren imaging optical setup

Flow visualization techniques like Schlieren and shadowgraphy are classically employed in the experimental analysis of such shock structures. For non-reacting species, Schlieren imaging is usually preferred and has been largely employed to investigate the aforementioned jet features [Hatanaka et al. 2012].

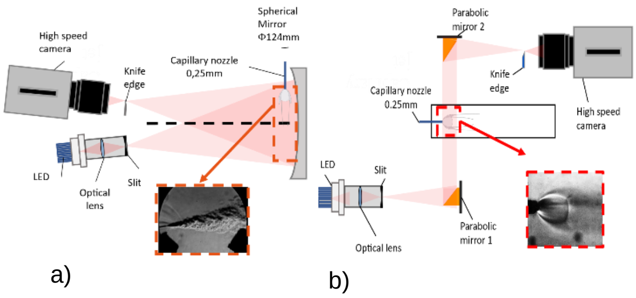

Fig. 2: Schematic of the optical Schlieren imaging setups a) Single spherical mirror setup b) Z-type with two parabolic mirrors setup

Various optical configuration can be setup for such purpose among which the so-called spherical mirror (*Fig. 2*a) is the most common for investigating far-field behaviors of jets and subsequent plumes (typically hundreds of the nozzle diameters) [Yeganeh eh al. 2023], while the so-called Z-type (*Fig. 2*b) is usually employed in near-fields studies (typically tens of the nozzle diameters) [Mahendiran 2025]. In the present study, both of these techniques are employed to address either short range shock structures and downstream behavior of the jet.

The obtained images are a result of the density gradient integrated along the optical path. The Schlieren imaging technique utilizes the phenomenon of light refraction to characterize the flow: the light passes through the expansion region, and the rays undergo refraction, resulting in a shift in the angle of incidence. Rays that do not undergo a change in angle proceed directly to the camera as a two-dimensional projection.

4 NEAR FIELD STRUCTURE OBSERVATIONS

4.1 NF structure and characterizing parameters

In the NF region, due to the high NPR considered in this study, complex physical phenomena occur, such as:

- The formation of a choked flow due to the high pressure ratio (NPR = 80 − 220). Exit velocity reaches M_e =1, nd an outward bended sonic line is form at the immediate nozzle exit.F
- The development of Prandtl-Meyer expansion fans (blue lines in Fig1) resulting from the under-expanded jet exiting into a lower ambient pressure. These isentropic expansions accelerate and turn the flow outward, increasing the Mach number above 1.
- The creation of shock structures: the barrel shock surrounding the supersonic jet core, the central Mach disk and the reflected wave. These are formed as the jet recompresses to ambient pressure. including a barrel shock surrounding the supersonic jet core and a central Mach disk.
- Joule-Thomson cooling due to isenthalpic expansion of sCO_2. This effect causes a local drop in temperature that affects the thermodynamic state of the flow.

All of these can explain the importance of the upstream conditions on the obtained jet structure and the necessity to understand and predict the structure of the near-nozzle area characterizing this type of flow.

The near-nozzle sonic characteristics are quantified by several important parameters that includes the dimensions of the Mach disk, the angle of the reflected shock at the triple-point. In the following sections, each of these parameters will be evaluated and compared to the literature values of highly under-expanded jets previously studied.

4.2 Mach disk position: Z_m

A commonly used empirical correlation has been proposed by Crist et al. [Crist et al. 1966] and provides a relation between the Mach disk length Z_m, the nozzle exit diameter d_c, and NPR. It has been experimentally obtained for diverging nozzles and NPR ranging from 20 to 200 that:

$$Z_m/d_e = C_{Z_m}\sqrt{NPR} \qquad (2)$$

Under such formalism, the Mach disk location Z_m is independent of the adiabatic ratio γ and thus weakly dependent of the fluid. It is indeed primarily governed by the pressure ratio and is therefore expected to produce a valid correlation of the conditions investigated here. C_{Z_m} is an experimentally determined constant and has been extensively studied in the literature [Franquet et al. 2015].

A commonly used experimental value of C_{Z_m} proposed by Ashkenas and Sherman [Ashkenas et al 1965] is 0.67, while Christ et al. [Crist et al. 1966]. proposed 0.645497 based on experimental investigations and an assumption of chocked condition at the nozzle exit ($M_e = 1$) and Young 0.69 for $\gamma = \frac{9}{7}$ [Young 1975]. Hatanaka [Hatanaka et al. 2012] found that the values of Z_m/d_e for a straight nozzle are smaller than those of other nozzles by about 25%.

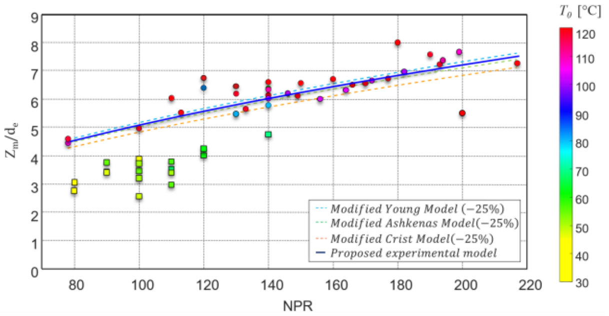

Fig. 3: Evolution of the Mach disk position as a function of the NPR for multiple temperature values. (Circles: single phase jet ; Squares: double phase jets)

Fig. 3 shows the three correlations plots modified and decreased by 25% as recommended by Hatanaka for straight nozzles, with the normalized experimental values of Z_m measured from the Schlieren images. Depending on P_0 and T_0 a single-phase or multiphase flow could be obtained, and for both considerations a comparison with the literature approaches was performed.

For a given pressure, if the upstream temperature is higher than a certain value, the flow only corresponds to a single-vapor phase (represented by red circles). The measured Z_m values fit the correlations found by Young [Young 1975], Christ et al [Crist et al. 1966] and Ashkenas [Ashkenas et al 1965] to predict the Mach disk position taking into account Hatanaka [Hatanaka et al. 2012] correction factor for straight nozzles when single phase expansion is represented. One can therefore conclude that the literature is relevant in evaluating the Z_m values assessed in this study although a exact value of $C_{Z_m} = 0.68$ is found from the regression of Eq. 2 on the actual data set.

Multiphase flows are represented by green squares in *Fig. 3* and appear for lower upstream temperatures. Under such condition, the previous correlations do not apply, literature studies are not available, and thus the Mach disk position could not be estimated nor predicted and previous findings are not reliable. In this case, the barrel shock is smaller than expected and dry ice particles modify the flow structure and its properties. This conclusion remains however to be confirmed for a wider range of experimental conditions and a larger experimental database. All in all, further investigations should be addressed prior to any definitive statement in this matter.

4.3 Mach disk diameter: D_m

The Mach disk diameter D_m is also an important parameter of the jet configuration, however it was clearly less investigated than the Mach disk length. Referring to Duronio et al. [Duronio et al. 2023], D_m is also mainly governed by the pressure ratio, is strongly dependent on the nozzle geometry and shape and is different for various gases.

Addy [Addy 1981] found that the diameters of different shaped jet nozzles are bounded by the following two empirical curves expressed by *Eq. 3* and represented in *Fig. 4:*.

$$D_m/d_e = 0.31\sqrt{NPR-5} \quad (3)$$

$$D_m/d_e = 0.36\sqrt{NPR-3.9}$$

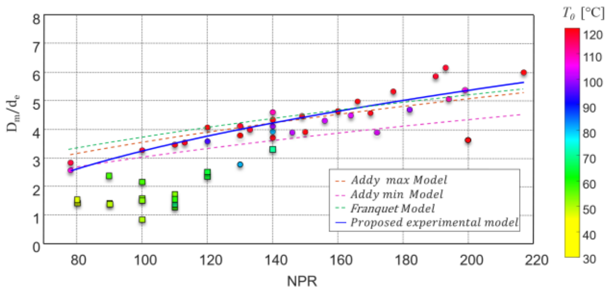

Fig. 4: Evolution of the Mach disk diameter as a function of the NPR for multiple temperature values.

Christ et al [Crist et al. 1966] stated that for high pressure ratios, normalized D_m shows the following dependency with the square root of the NPR:

$$D_m/d_e = C_{D_M}\sqrt{NPR} \quad (4)$$

Taking into consideration the previous findings, Franquet et al [Franquet et al. 2015] found C_{D_m} equal to 0.37 (green dashed line). *Fig. 4* shows that the Mach disk diameter measured by the Schlieren images for various NPR and temperatures are in a good agreement with Addys bounded region for NPR lower than 150, and have higher values for NPR above 150. Franquet correlation represents a better fit for high NPR values than Addy but has not good predictions for low pressure ratio.

$$D_m/d_e = C_{D_M}\sqrt{NPR-b} \quad (5)$$

The best fit for the obtained experimental values all over the pressure and temperature range evaluated is represented in blue solid line for *Eq. 5* with 0.106 and 42.87 values obtained for C_{D_m} and b respectively, by optimizing this function for the different test values.

However, it is also important to insist that these expressions are for a single-phase flow and do not apply for multiphase conditions. Correlations found in here and in literature are not reliable when carbonic ice is present in the flow and further studies have to be conducted if optimal conditions in machining were found to be when multiphase flow is produced.

4.4 Barrel shock area evolution with NPR

As discussed in the previous sections, the dimensions of the barrel structure are strongly dependent on the upstream conditions P_0 and T_0, and the flow phase content.

This dynamic zone dictates how the jet expands and interacts with its surroundings, strongly influencing the way heat is exchanged with the target surface.

In machining, the targeted surface may be very close to the nozzle exit (as in drilling). Under such conditions, the impinged surface intersects the near field structures. It is in the stagnation region (facing the Mach disk) that the heat transfer coefficient (HTC) is observed to be at its maximum [Masson et al. 2025], due to the important gradients in this part of the jet.

As highlighted in *Fig. 5*, when the NPR increases, the size of the barrel shock increases, resulting in a wider jet and a larger stagnation region on the machined surface. This results in an increased thermal interaction area where the high temperature gradients across the barrel shock can be more effective in heat removal.

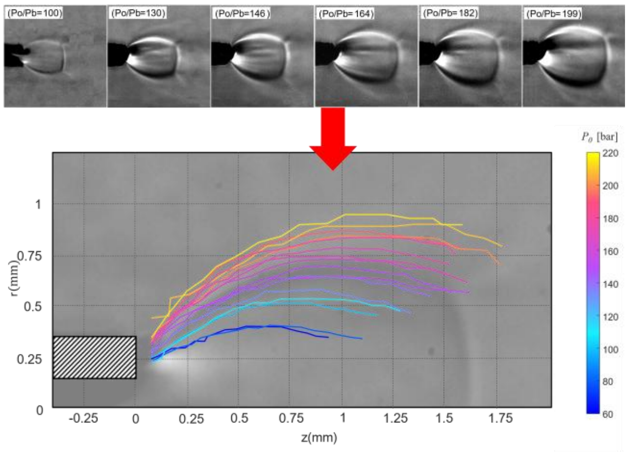

Fig. 5 : Plot of the evolution of the barrel shock curvature obtained from the schlieren images at a constant temperature of T=120°C for multiple pressure values

All in all, the volume of the barrel structure depicted in Fig. 6 is observed to follow a linear trend with respect to NPR.

Accordingly, a linear correlation is proposed in Fig. 6 between the calculated volume and the NPR, where the volume is obtained by revolving the surface defined by the experimental curves in Fig. 5 around the Z-axis. The resulting linear expression is:

$$V = a\,NPR + b \quad (6)$$

with 0.023 and 1.4684 respectively the values of a and b.

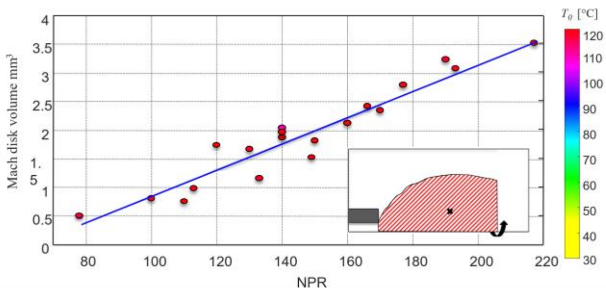

Fig. 6 : Evolution of the Barrel shock structure volume in function of the NPR values

The model confirms a linear dependency between NPR and the barrel shock volume. Using this correlation, the volume of the barrel shock structure can be predicted, where the largest temperature and pressure gradients are located.

5 JET STRUCTURE FOR SHORT RANGE IMPINGEMENT

When impinged, the sCO_2 jet structures may be intersected by the target, especially at closer ranges. As stated by the experimental work of Masson et al., the heat transferred from the fluid to the surface is a prime function of the nozzle-to-plate distance D_{PL} and decreases along with it. At a shorter range (D_{PL}/de < 20) the heat transfer coefficient experiences what seems an erratic decrease while at longer ranges (beyond D_{PL}/de = 40) the natural decay of the heat transfer capacity follows a $1/D_{PL}$ classical law.

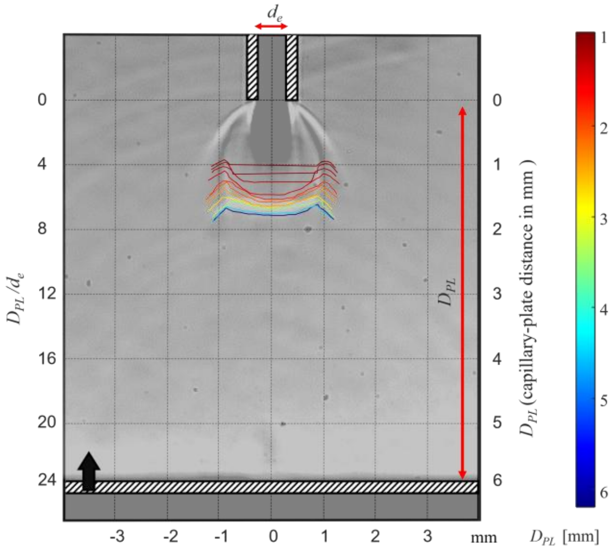

Fig. 7: Mach disk sonic line and triple point angle curvature in function of the nozzle to plate distance obtained by schlieren images processing

From the near-field Schlieren observation of the present contribution, it is possible to draw some conclusions regarding such behaviour. First, as seen in Fig.7, the shock structures of the jet are fairly unaffected for impingement distance above D_{PL}/de >10 when the bending of the Mach disk becomes observable. At such distances, the stagnation region is known to be prone to fluid recirculation [Alvi 2002]. This phenomenon is a known feature of the under-expanded jet impingements [Kim 2019] and is associated with a lower heat transfer capacity since recirculation prevents from cold gas to come in contact with the plate. If recirculation is not involved, then the heat transfer is mainly affected by the velocity decay due to laminar/turbulent transition which occurs when D_{PL} increases. Again, the dissipative nature of a turbulent flow is classically fit by a $1/D_{PL}$ decay law [Papadopoulos 1999] which then fully explain the cooling decrease observed by Masson et al.

At closer distances (typ. D_{PL}/de <10) the Mach disk starts to bend toward the plate thus imparting an outgoing motion to the fluid. Under such condition, recirculation is made impossible and the fluid starts to separate the plate boundary layer. A such distance the jet may reach its optimal cooling capacity. Indeed, the length beyond the Mach disk is long enough for the decompression of the gas to be completed and thus yields a minimal jet temperature from the Joule-Thompson effect and the jet regime is laminar thus preventing from mixing with warmer ambient air.

The shock structure further evolves for D_{PL}/de <4 (see Fig.7). The Mach disk reflects on the plate forming a structure known as “a plate disk” which is clearly observable for such configurations. Conversely to the results obtained by Lamont and Hunts [Lamont 1980] for smaller NPR, the plate disk remains flat all the way down to D_{PL}/de =1. No recirculation bubble is observed nor any bump on the plate disk. From the observed Schlieren images of the jet structure it appears that the jet is somewhat pinched thus creating a “circumferential nozzle” though no radial shock wave is observed. The stagnation region of the impingement corresponds to the recompression zone, the region located in the immediate downstream of the Mach disk. This latter is in direct contact with the plate, suggesting that the jet pressure is not close to the ambient and thus that the jet temperature remains is closer to T_0 than T_∞ (where T_∞ is the ambient temperature).

It is worth mentioning that if solid carbon dioxide is formed during the decompression process the shape of the barrel structure is strongly affected (see above) and therefore the present considerations should be modified accordingly. Hence, the short-range impingement of such shock structure and the subsequent heat transfer can be seen as strictly dependent of the barrel shape.

6 SUMMARY

This paper intends to address the behavior of a free and impinged sCO_2 jet structure and its geometrical evolution in function of the upstream jet conditions. The supersonic structure and parameters were analyzed under varying initial pressures and temperatures in both near and far fields. The structure of the under-expanded supercritical CO_2 jet is primarily governed by upstream pressure and temperature. Single-phase conditions yield consistent shock patterns, for which established correlations can predict key features such as Mach disk location and diameter. In contrast, multiphase flow, particularly with the formation of solid CO_2, significantly alters the jet geometry and reduces prediction accuracy. Near-field Schlieren observations reveal that the shock structure evolves as the jet approaches the surface. At close distances, recirculation is suppressed, the boundary layer is disrupted, and optimal cooling occurs due to complete gas decompression and limited mixing with the ambient. When solid CO_2 is present, the barrel shock structure is modified, which affects the heat transfer behavior. Overall, the cooling performance is closely linked to the jet structure, which depends on the flow regime and upstream conditions.

7 REFERENCES

[Addy 1981] Addy, A.L. Effects of axisymmetric sonic nozzle geometry on Mach disk characteristics. AIAA Journal, January 1981, Vol.19, No.1, 121-122.

[Alvi 2002] Alvi, F.S., et al. Experimental and Computational Investigation of Supersonic Impinging Jets. AIAA Journal, April 2002, Vol.40, No.4,599-609.

[Ashkenas et al. 1965] Ashkenas, H. and Sherman, F. The Structure and Utilization of Supersonic Free Jets in Low Density Wind Tunnels. Rarefied Gas Dynamics 1965, No.2,84-105

[Crist et al. 1966] Crist, S. et al. Study of the highly underexpanded sonic jet. AIAA Journal, January 1966, Vol.4, No. 1, 68–71.

[Duronio et al. 2023] Duronio, F. et al. Under-Expanded Jets in Advanced Propulsion Systems—A Review of Latest Theoretical and Experimental Research Activities. Energies, September 2023, Vol16, No.18, 6471

[Franquet et al. 2015] Franquet, E. et al. Free underexpanded jets in a quiescent medium: A Review. August 2015, Vol.77, 25-53.

[Hatanaka 2012] Hatanaka, K. and Saito, T. Influence of nozzle geometry on underexpanded axisymmetric free jet characteristics, Shock Waves, 2012, Vol. 22, No.5, 427-434.

[Kim 2019] Kim, D. and Lee, J. Influence of shock structure on heat transfer characteristics in supersonic under-expanded impinging jets. International Journal of Thermal Sciences, July 2019, Vol.141, 62-71.

[Koulekpa 2023] Koulekpa, K.S. et al. Analysis of CO2 Jet's Temperature by BOS Method for Applications in Cryogenic Machining. 23rd Machining Innovations Conference for Aerospace Industry 2023, Germany. SSRN Electronic Journal, 2023.

[Lamont 1980] Lamont, P. J., Hunt, B. L. The impingement of underexpanded, axisymmetric jets on perpendicular and inclined flat plates. Journal of Fluid Mechanics, 1980, Vol. 100, 471-511.

[Mahendiran 2025] Mahendiran, S. and Sridhar, B.T.N. Near field features of orthogonally impinging underexpanded triangular and hexagonal supersonic jets. Acta Astronautica, March 2025, Vol.228, 204-223.

[Masson et al. 2025] Masson, P. et al. Thermal investigations of supercritical CO_2 jet impingement and its cooling applicability in a machining context. International Journal of Heat and Mass Transfer, January 2025, Vol.236, 126335.

[Papadopoulos 1999] Papadopoulos, G., William, M.P. A Generic Centerline Velocity Decay Curve for Initially Turbulent Axisymmetric Jets. Papadopoulos, George; Pitts, William M. Journal of Fluids Engineering, 1999, Vol. 121, 80-85.

[Supekar et al. 2012] Supekar, S.D. et al. Performance of supercritical carbon dioxide sprays as coolants and lubricants in representative metalworking operations. Journal of Materials Processing Technology, December 2012, Vol.212, 2652-2658.

[Yeganeh et al. 2023] Yeganeh, M. et al. Visualization and comparison of methane and hydrogen jet dynamics using schlieren imaging. Fuel, January 2023, Vol. 331, 125762.

[Young 1975] Young, W.S. Derivation of the free jet Mach disk location using the entropy balance principle. The Physics of Fluids, 1975, Vol. 12, 1421-1425.